## References and Notes

(1) Ober, C. K.; Jin, J. I.; Lenz, R. W. *Adv. Polym. Sci.* **1984**, *59*, 130.
(2) Finkelmann, H. *Angew. Chem., Int. Ed. Engl.* **1987**, *26*, 816.
(3) Ringsdorf, H.; Schlarb, B.; Venzmer, J. *Angew. Chem., Int. Ed. Engl.* **1988**, *27*, 113.
(4) Blumstein, R. B.; Blumstein, A. *Mol. Cryst. Liq. Cryst.* **1988**, *165*, 361.
(5) Noel, C. *Makromol. Chem., Macromol. Symp.* **1988**, *22*, 95.
(6) Economy, J. *Mol. Cryst. Liq. Cryst.* **1989**, *169*, 1.
(7) Jackson, W. J., Jr. *Mol. Cryst. Liq. Cryst.* **1989**, *169*, 23.
(8) Ballauff, M. *Angew. Chem., Int. Ed. Engl.* **1989**, *28*, 253.
(9) Demus, D. *Liq. Cryst.* **1989**, *5*, 75.
(10) Percec, V.; Yourd, R. *Macromolecules* **1988**, *21*, 3379.
(11) Percec, V.; Yourd, R. *Macromolecules* **1989**, *22*, 524.
(12) Percec, V.; Yourd, R. *Macromolecules* **1989**, *22*, 3229.
(13) Percec, V.; Yourd, R. *Makromol. Chem.* **1990**, *191*, 25.
(14) Percec, V.; Yourd, R. *Makromol. Chem.* **1990**, *191*, 49.
(15) Percec, V.; Tsuda, Y. *Macromolecules* **1990**, *23*, 5.
(16) Percec, V.; Tsuda, Y. *Polym. Bull.* **1989**, *22*, 489.
(17) Percec, V.; Tsuda, Y. *Polym. Bull.* **1989**, *22*, 497.
(18) Percec, V.; Tsuda, Y. *Polym. Bull.* **1990**, *23*, 225.
(19) Percec, V.; Keller, A. *Macromolecules*, submitted.
(20) Ungar, G.; Feijoo, J. L.; Keller, A.; Yourd, R.; Percec, V. *Macromolecules*, in press.
(21) Cheng, S. Z. D.; Yandrasits, M. A.; Percec, V. *Polymer*, in press.
(22) Ronca, G.; Yoon, D. Y. *J. Chem. Phys.* **1982**, *76*, 3295.
(23) Chuit, P. *Helv. Chim. Acta* **1929**, *9*, 271.
(24) Chuit, P.; Hansser, J. *Helv. Chim Acta* **1932**, *12*, 850.
(25) Hunig, S.; Lucke, E.; Brenninger, W. *Organic Synthesis*; Baumgarten, H. E., Ed.; Wiley: New York, 1973; Collect. Vol. V, p 533.
(26) Demus, D.; Richter, L. *Texture of Liquid Crystals*; Verlag Chemie: Weinheim, 1978.
(27) Percec, V.; Nava, H. *J. Polym. Sci., Polym. Chem. Ed.* **1987**, *25*, 405.
(28) Percec, V.; Nava, H. *J. Polym. Sci., Polym. Chem. Ed.* **1987**, *25*, 1943.
(29) Vasilenko, S. V.; Khokhlov, A. R.; Shibaev, V. P. *Macromolecules* **1984**, *17*, 2270.
(30) Blumstein, A.; Thomas, O. *Macromolecules* **1982**, *15*, 1264.
(31) Blumstein, A. *Polym. J.* **1985**, *17*, 277.
(32) Kumar, R. S.; Clough, S. B.; Blumstein, A. *Mol. Cryst. Liq. Cryst.* **1988**, *157*, 387.
(33) Roviello, A.; Sirigu, A. *Makromol. Chem.* **1982**, *183*, 895.
(34) Strzelecki, L.; Liebert, L. *Eur. Polym. J.* **1981**, *17*, 1271.
(35) Jin, J. I.; Choi, E. J.; Ryu, S. C.; Lenz, R. W. *Polym. J.* **1986**, *18*, 63.
(36) Jin, J. I.; Park, J. H. *Mol. Cryst. Liq. Cryst.* **1984**, *110*, 293.
(37) Buglione, J. A.; Roviello, A.; Sirigu, A. *Mol. Cryst. Liq. Cryst.* **1984**, *106*, 169.
(38) Emsley, J. W.; Luckhurst, G. R.; Shilstone, G. N.; Sage, I. *Mol. Cryst. Liq. Cryst. Lett.* **1984**, *102*, 223.
(39) Griffin, A. C.; Vaidya, S. R.; Hung, R. S. L.; Gorman, S. *Mol. Cryst. Liq. Cryst. Lett.* **1985**, *1*, 131.
(40) Jin, J. I.; Oh, H. T.; Park, J. H. *J. Chem. Soc., Perkin Trans. 2* **1986**, 343.
(41) Imrie, C. T. *Liq. Cryst.* **1989**, *6*, 391.
(42) Yoon, D. Y.; Baumgartner, A. *Macromolecules* **1984**, *17*, 2864.
(43) Yoon, D. Y.; Bruckner, S. *Macromolecules* **1985**, *18*, 651.
(44) Yoon, D. Y.; Bruckner, S.; Volksen, W.; Scott, J. A.; Griffin, A. C. *Faraday Discuss., Chem. Soc.* **1985**, *79*, 41.
(45) Abe, A. *Macromolecules* **1984**, *17*, 2280.
(46) Gray, G. W. *Molecular Structure and the Properties of Liquid Crystals*; Academic Press: London and New York, 1962; p 148.
(47) Percec, V.; Tsuda, Y., to be published.

---

# Carbon-13 Nuclear Magnetic Resonance Measurements of Local Segmental Dynamics of Polyisoprene in Dilute Solution: Nonlinear Viscosity Dependence

**S. Glowinkowski,[†] Daniel J. Gisser, and M. D. Ediger***

*Department of Chemistry, University of Wisconsin, Madison, Wisconsin 53706*

*Received November 21, 1989; Revised Manuscript Received February 6, 1990*

ABSTRACT: The local segmental dynamics of polyisoprene in dilute solution have been studied with natural-abundance $^{13}$C NMR spectroscopy. Ten solvents covering a factor of 70 in viscosity were utilized. Correlation times ($\tau_c$) extracted from $T_1$ measurements were determined as a function of temperature in all solvents. Contrary to the predictions of Kramers' theory in the high friction limit, it was found that $\tau_c \propto \eta^{0.41\pm0.02}$ at constant temperature. The potential barrier height for local dynamics extracted from these measurements is 13 ± 2 kJ/mol. The use of Kramers' theory to extract this barrier height leads to serious errors and nonphysical results. The results are discussed in terms of Grote–Hynes theory in which the friction opposing conformational transitions is frequency dependent. Ratios of $nT_1$ values for methine and methylene carbons are independent of solvent and not equal to unity.

## Introduction

The local segmental dynamics of polymer chains have an important influence on the macroscopic properties of polymeric systems. In polymer solutions where local dynamics occur on picosecond and nanosecond time scales, this influence is mainly through the larger distance scale motions, which dominate ordinary viscoelastic properties under these conditions. Dynamics on the length scale of a few monomer units depend strongly on the details of the monomer structure. Hence information about local segmental dynamics provides an important intermediate link between molecular structure and larger motions. In a polymer melt near $T_g$, the time scales for local conformational transitions slow significantly. Dynamics on the scale of a few monomer units are intimately connected with the main glass transition in many polymers.

---

[†] On leave from the Institute of Physics, A. Mickiewicz University, Poznan, Poland.

* Author to whom correspondence should be addressed.

0024-9297/90/2223-3520$02.50/0

Certain types of local segmental dynamics can also directly influence material properties in the sub-$T_g$ region.

Our group[1,2] and others[3,4] have used time-resolved optical spectroscopy of chains labeled with chromophores to investigate local segmental dynamics. In work recently published we investigated the molecular weight and solvent dependence of the local dynamics of polyisoprene in dilute solution.[1] Those experiments indicated that the thermodynamic quality of the solvent plays a significant role in determining the local dynamics observed by the optical experiments but that no important role was played by specific polymer/solvent interactions. For good solvents, only the temperature and viscosity need to be specified in order to predict the local dynamics.

The present work was motivated in part by a desire to compare NMR measurements with the optical measurements described above. The NMR and optical techniques are complementary. The optical experiments provide a direct measurement of an orientation autocorrelation function involved in local motions but require the presence of a fairly bulky chromophore in the chain backbone. The NMR experiments do not require perturbative labeling schemes but only provide indirect information about the correlation functions that characterize the local dynamics. No detailed study of the local dynamics in solutions of polyisoprene using NMR has been published up to this point. Two groups have recently published investigations of bulk polyisoprene using $^{13}$C NMR.[5,6]

A second goal of the present work was to examine the local segmental dynamics of polyisoprene in solvents with a wide range of viscosities. There seems to be a general consensus in the literature that correlation times increase with solvent viscosity, but the functional form of this dependence is not settled from an experimental perspective.[1,4,7-10] Among NMR studies, only two groups have tested the relationship between correlation time and viscosity over a wide range of viscosities. Both of these studies used poly(ethylene oxide).[9,10] In our measurements we were particularly interested in using highly viscous solvents, such as Aroclor 1248, which are often used in mechanical measurements of polymer dynamics in solution. The present work may contribute to the understanding of the anomalous high-frequency behavior seen in dynamic mechanical measurements of polymers in viscous solvents.[11]

Finally, it has previously been reported that polyisoprene does not obey the "$nT_1$ rule".[5,12] This implies that different C–H vectors in the chain backbone have different motional characteristics. In this study we use this information about motion within the repeat unit to investigate the role of the solvent in local dynamics.

The results of this study are surprising. Kramers' theory,[13,14] which is almost universally assumed to be the appropriate framework for discussing local polymer dynamics in solution, cannot describe our results. A generalized version of Kramers' theory by Grote and Hynes[15] rationalizes our results and allows us to connect the results from this NMR study with the results from the optical study that stimulated this work. The Grote–Hynes theory starts from the generalized Langevin equation, which allows consideration of the frequency dependence of the friction opposing conformational transitions. One consequence of these results is that potential energy barriers for local dynamics reported in the literature may be seriously in error. All of our results are consistent with a continuum view of the solvent in which specific polymer/solvent interactions are not important.

**Table I**
**Polyisoprene Characterization**

| source | $M_w$ | $M_w/M_n$ | cis-1,4, % | trans-1,4, % | vinyl-3,4, % |
|---|---|---|---|---|---|
| Goodyear | 10 200 | 1.11 | 76 | 18 | 6 |
| Polysciences | 10 200 | 1.11 | 68 | 27 | 5 |
| Polysciences | 290 000 | 1.04 | 80 | 16 | 4 |

## Experimental Section

**Materials.** We have measured natural-abundance $^{13}$C spin–lattice relaxation times, $T_1$, in dilute solutions of polyisoprene in 10 solvents. Three polyisoprene samples were used (see Table I). Although the two low molecular weight polymers had slightly different microstructures, they displayed no significant differences in these experiments and were used interchangably.

The solvents used are listed in Table II. All nondeuterated solvents were obtained from Aldrich except for chloroform (EM-Science) and Aroclor 1248 (Monsanto Chemical Co., Lot No. KM502). For some experiments, we used perdeuterated toluene [Aldrich and Cambridge Isotope Laboratories (CIL)] and cyclohexane (CIL). The solvents were greater than 99% purity except for 2-pentanone (97%) and 1,1,2,2-tetrachloroethane (98%). They were used as received except for 2-pentanone, which was filtered twice with activated charcoal.

Solvents were selected to encompass a wide range of viscosity, thermodynamic quality, and molecular structure. At 333 K the solvents span a factor of 46 in viscosity while at 310 K they span a factor of 150. Toluene, tetrachloroethane, and cyclohexane are good solvents,[16,17] hexadecane is a moderately good solvent,[18] while 2-pentanone and 1,4-dioxane are $\Theta$ solvents ($\Theta \approx 307$ K for this microstructure in both solvents).[19] Squalane is a fully hydrogenated linear hexamer of isoprene. Aroclor 1248 is a highly viscous mixture of polychlorinated biphenyls. The exact composition of the mixture is unknown but contains 48% chlorine by weight (3.9 chlorine atoms/molecule).

**Solvent Viscosity.** Table II presents viscosity equations for the solvents used. Except for squalane, these data were obtained from the literature. The viscosity of squalane was measured by using Cannon–Fenske capillary flow viscometers at five temperatures between 273 and 344 K. Additionally, the viscosities of toluene-$d_8$ and cyclohexane-$d_{12}$ were measured. We found that deuteration of toluene and cyclohexane did not change the viscosity within experimental uncertainty (1%) between 280 and 326 K.

The viscosity of Aroclor 1248 (Lot No. KM502) has been well characterized between 261 and 318 K.[20,21] It is difficult to extrapolate these data to the higher temperatures we have studied. Harris has reported the viscosity of Aroclor 1248 over a much wider temperature range.[22] The two sets of measurements agree within 5–10% over the range where they overlap. We have used the Harris measurements to analyze our data and a fit to these data is given in Table II.

**Solution Preparation.** All NMR measurements were made on 9.7 ± 0.3% (w/w) solutions of polyisoprene. Several authors have shown that $^{13}$C spin–lattice relaxation times of synthetic polymers in dilute solution are independent of concentration below about 15% polymer,[23] so we assume that our measurements accurately reflect dilute solution properties. Solutions were passed through a 0.45-$\mu$m filter to remove any cross-linked or very high molecular weight material.

Dissolved oxygen can provide an undesired pathway for spin–lattice relaxation. This mechanism is not expected to be important for $^{13}$C nuclei with $T_1$s less than approximately 5 s,[24,25] as was the case for backbone carbon nuclei. Most solutions were degassed by using several freeze–pump–thaw cycles. Some solutions became irreversibly cloudy during this procedure, so identical solutions were prepared without degassing. Polyisoprene spin–lattice relaxation times of samples that had not been degassed were the same as for samples that had been degassed. Solvent $T_1$s often were much longer than 5 s, so we report measurements of solvent $T_1$ values only for degassed samples.

Another undesired source of magnetic relaxation is dipole–dipole coupling with solvent nuclei, particularly protons, which are abundant and have a large magnetic moment. Deuterated

**Table II**
**Solvent Viscosities**

| solvent | ref | eq | temp range, K | *A* | *B* | *C* |
|---|---|---|---|---|---|---|
| 2-pentanone | 75 | 1 | 273-373 | 5154.3 | -135.40 | 1.8248 |
| toluene | 75 | 1 | 273-380 | 1895.4 | -160.16 | 1.6522 |
| toluene | 76 | 3 | 155-288 | -1.1560 | -177.85 | 103.1 |
| chloroform | 77 | 3 | 210-360 | -1.4573 | -325.76 | 23.789 |
| cyclohexane | 77 | 2 | 280-360 | -2.1466 | 625.44 | |
| 1,4-dioxane[a] | 78 | 2 | 283-353 | -2.1142 | 652.51 | |
| tetrachloroethane[a] | 75 | 3 | 273-353 | -1.5161 | -406.04 | 63.47 |
| *n*-hexadecane | 77 | 3 | 290-520 | -1.8174 | -578.33 | 46.605 |
| *cis*-decalin | 77 | 3 | 240-460 | -1.4480 | -395.48 | 93.359 |
| squalane[a] | | 3 | 273-344 | -1.0766 | -324.62 | 169.27 |
| Aroclor 1248[a] | 22 | 3 | 294-360 | -0.6121 | -165.62 | 241.06 |

equations ($\eta$ in centipoise, $T$ in Kelvin)
(1) $\eta = A(B + T)^{-C}$
(2) $\log \eta = A + B/T$
(3) $\log \eta = A + B/(C - T)$

[a] Parameters in equation fit by authors. Equations fit data within 1% for 1,1,2,2-tetrachloroethane and squalane and within 4% for 1,4-dioxane and Aroclor 1248.

solvents are commonly used to circumvent this problem. Since the importance of dipole-dipole relaxation diminishes with the sixth power of the distance separating the two nuclei, $^{13}C$ relaxation is dominated by directly bonded protons and contributions from solvent protons should be minimal. Indeed this was found to be the case. Polyisoprene $T_1$s in toluene and cyclohexane were not affected by solvent deuteration. For the other solvents, we assume that contributions to polyisoprene $T_1$ relaxation by solvent protons were negligible.

**NMR Measurements.** The labeling scheme used to identify the five carbon atoms in the polyisoprene repeat unit is

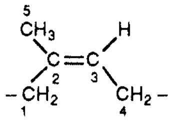

The $^{13}C$ NMR spectrum of polyisoprene has been assigned previously.[26,27] The different sequences of cis-1,4, trans-1,4, and vinyl-3,4 produce a series of $^{13}C$ resonances for each of the carbon atoms. We have measured $T_1$s for the most intense line of each series, in each case corresponding to carbon atoms in cis-1,4 linkages. These lines occur at 32 ppm for C1, 125 ppm for C3, and 26 ppm for C4. We have not analyzed $T_1$s for carbons C2 and C5 because we wish to restrict our attention to backbone carbons where dipole-dipole interaction with bonded protons is the dominant relaxation mechanism.

$^{13}C$ NMR spectra were recorded by using composite pulse (WALTZ-16) proton decoupling.[28] $CDCl_3$ or dimethyl-$d_6$ sulfoxide in an outer NMR tube provided a deuterium signal for locking. Most measurements were made at a $^{13}C$ Larmor frequency of 90.6 MHz on a Bruker AM-360. Measurements were also made at 125.8, 67.9, and 25.2 MHz by using Bruker AM-500, WP-270, and AC-100 spectrometers, respectively. Spin-lattice relaxation times were measured with the inversion-recovery ($\pi$-$t$-$\pi/2$-FID)$_n$ pulse sequence. Spectra were collected by using at least eight delay times $t$ and waiting at least eight times $T_1$ between acquisitions. $T_1$ values were computed from three-parameter fitting and sometimes additionally from the slope of $\ln (M_0 - M_z)$ as a function of $t$. In all cases the recovery of magnetization was well described by a single exponential, even when as many as 20 decay times were used. Nuclear Overhauser enhancements (NOE) were measured by comparing $^{13}C$ peak intensities for spectra acquired by using continuous $^1H$ decoupling and inverse gated decoupling, waiting more than 10 $T_1$ between acquisitions. The sample temperature was controlled within 1 K. $T_1$ values are believed accurate within 10% and NOEs within 15%.

## Analysis of NMR Measurements

Several mechanisms may contribute to the spin relaxation of $^{13}C$ nuclei. In polymers the dominant process is generally the $^{13}C$-$^1H$ dipole-dipole interaction.[29,30] In the previous section we have argued that for these experiments only interactions with bonded protons need be considered. Under conditions of complete proton decoupling and if cross-relaxation effects between bonded protons are negligible, the $^{13}C$ spin-lattice relaxation time $T_1$, spin-spin relaxation time $T_2$, and nuclear Overhauser enhancement (NOE) may be written in terms of the spectral density function, $J(\omega)$[23,29-31]

$$\frac{1}{T_1} = Kn[J(\omega_H-\omega_C) + 3J(\omega_C) + 6J(\omega_H+\omega_C)] \qquad (1)$$

$$\frac{1}{T_2} = \frac{1}{2T_1} + \frac{Kn}{2}[4J(0) + 6J(\omega_H)] \qquad (2)$$

$$\text{NOE} = 1 + \frac{\gamma_H}{\gamma_C}\left[\frac{6J(\omega_H+\omega_C) - J(\omega_H-\omega_C)}{J(\omega_H-\omega_C) + 3J(\omega_C) + 6J(\omega_H+\omega_C)}\right] \qquad (3)$$

where $\gamma_C$ and $\gamma_H$ are the gyromagnetic ratios for carbon and hydrogen, $\omega_C$ and $\omega_H$ are their resonance frequencies, and $n$ is the number of bonded protons. The constant $K$ and $J(\omega)$ are defined as

$$K = \frac{1}{10}\left[\frac{\mu_0\gamma_H\gamma_C\hbar}{4\pi r^3}\right]^2 = 2.15 \times 10^9\ \text{s}^{-2} \qquad (4)$$

$$J(\omega) = \frac{1}{2}\int_{-\infty}^{+\infty} G(t)\, e^{i\omega t}\, dt \qquad (5)$$

where $r$ is the carbon-hydrogen internuclear distance (taken to be 1.09 Å for methine and methylene carbons). $G(t)$ is the second-order orientation autocorrelation function of a C-H bond:

$$G(t) = (1/2)\langle 3(\mathbf{e}_x(0)\cdot\mathbf{e}_x(t))^2 - 1\rangle \qquad (6)$$

In this equation, $\mathbf{e}_x(t)$ is a unit vector in the direction of the C-H bond at time $t$. The brackets indicate an ensemble average.

Often $G(t)$ is not a single exponential and contains a distribution of time constants $\tau$, which describe molecular motion. When the extreme narrowing condition

$$(\omega_H + \omega_C)\tau \ll 1 \qquad (7)$$

is fulfilled for all $\tau$ that contribute to $G(t)$, then eqs 1-3 simplify to

$$1/T_1 = 1/T_2 = 10nK\tau_c \qquad (8)$$

$$\text{NOE} = 1 + \gamma_H/2\gamma_C \cong 2.99 \qquad (9)$$

The correlation time $\tau_c$ in eq 8 is simply the integral of

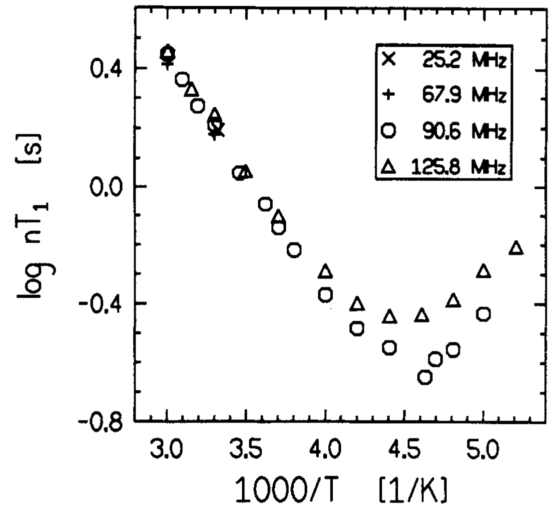

**Figure 1.** Temperature dependence of spin–lattice relaxation time, $nT_1$, for methylene carbon C4 at 90.6 and 125.8 MHz. A few points for 25.2 and 67.9 MHz are also included. The sample is 10% polyisoprene (10K) in toluene-$d_8$.

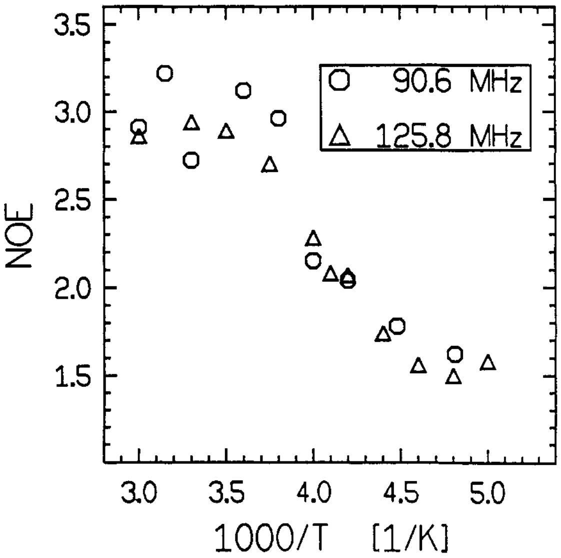

**Figure 2.** Temperature dependence of NOE measured at 90.6 and 125.8 MHz for methylene carbon C4 of 10K polyisoprene in toluene-$d_8$.

the correlation function:[32,33]

$$\tau_c = \int_0^\infty G(t)\, dt \qquad (10)$$

Therefore, in the extreme narrowing regime the spin–lattice and spin–spin relaxation times are equal to each other, are independent of the Larmor frequency, and can be easily related to $\tau_c$. The correlation time characterizes the rotational motion of a C–H bond.

Figure 1 shows the temperature dependence of the $^{13}$C spin–lattice relaxation time $nT_1$ for the methylene carbon C4 of 10K polyisoprene in toluene. Most of the points are at resonance frequencies of 90.6 or 125.8 MHz, with a few included for 67.9 and 25.2 MHz. As shown in the figure, $T_1$ is independent of Larmor frequency over a substantial range of temperature (260–333 K). NOE measurements for C4 are shown in Figure 2. At temperatures above 260 K for the 90.6-MHz data and above 275 K for the 125.8-MHz data the NOEs are close to 3.0. The other two backbone carbons, C1 and C3, display similar $T_1$ and NOE behavior.

Both of the above observations are consistent with the extreme narrowing conditions. The remaining requirement is that $T_1 = T_2$, as was stated in eq 8. Dynamic measurements of the spin–spin relaxation times $T_2$ (using the CPMG pulse sequence[34,35]) at 125.8 MHz show that $T_2$ has the same temperature dependence as $T_1$ but generally is about half as long. Thus our observations do not strictly indicate extreme narrowing.

We can interpret the results above in a manner suggested by English and Dybowski[36] and by Schaefer,[37] on the basis of studies of motions in bulk polybutadiene and polyisoprene. Fast local motions *almost* completely randomize the orientation of a given C–H vector in polyisoprene. However, very slow long-range motions (perhaps end-over-end motions) are required to completely randomize this orientation. Qualitatively we can write[38]

$$G(t) = aG_0(t) + (1 - a)G_i(t) \qquad (11)$$

where $G_0(t)$ represents a slowly decaying part of the correlation function, $G_i(t)$ represents that part of the correlation function determined by internal dynamics, and $a \ll 1$. The fact that $T_1$ is independent of Larmor frequency over a range of temperatures indicates that there is a separation in time scales between the decays of $G_0(t)$ and $G_i(t)$. Using the data in Figures 1 and 2 and the fact that $2T_2 \approx T_1$, we estimate that $a < 0.005$ and that the separation in time scales between the two types of decay processes is at least 3 decades.

In this paper we have used eq 8 to obtain $\tau_c$ from $T_1$ in the temperature region where $T_1$ is independent of the Larmor frequency. The correlation time we extract from this procedure is actually an effective correlation time, which is the integral of $G_i(t)$, the fast part of the correlation function. For the remainder of this paper we refer to this effective correlation time as $\tau_c$.

Many attempts have been made to find a form of the correlation function that quantitatively describes $^{13}$C relaxation data.[30] Single-exponential correlation functions,[9,39,40] nonexponential correlation functions,[41–44] and distributions of correlation times[30,45] have all been used with varying degrees of success. The correlation time defined in the manner discussed above is independent of the shape of $G_i(t)$. It characterizes the reorientation of the vector of interest (the C–H bond in our experiments) without reference to a specific motional model. If more than one type of motion is responsible for the reorientation of the appropriate vector, then the motion cannot be well characterized by a single-exponential correlation function and $\tau_c$ is an appropriately weighted average of the time constants that enter into a microscopic description of the motion.[38] Note that this definition of $\tau_c$ differs from the way $\tau_c$ is sometimes used in the NMR literature.

It is possible that mechanisms other than dipole–dipole relaxation may influence spin dynamics. In particular, chemical shift anisotropy (CSA) may be an efficient relaxation mechanism at the rather large magnetic fields we have used. A differential line-broadening experiment[46] at a $^{13}$C resonance frequency of 125.8 MHz indicated that the CSA for the methine carbon (C3) of polyisoprene in toluene is about 150 ppm. The CSA contribution to experimental $T_1$ relaxation therefore is negligible, below 5% for 90.6-MHz measurements.[29] The CSA for the methylene groups is much smaller[47] and also negligible.

Only for the solvent toluene have we measured NOEs and the dependence of $T_1$ upon Larmor frequency. For the remaining solvents, $T_1$ measurements were made at 90.6 MHz only. We assume that the procedure described above for extracting $\tau_c$ from $T_1$ is valid as long as the data indicate that we are on the extreme narrowing side of the $T_1$ minimum, and $nT_1$ is greater than 0.4 s for

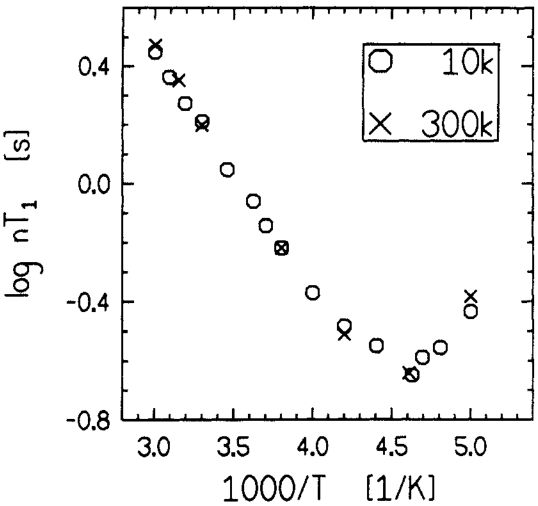

**Figure 3.** Temperature dependence of $nT_1$ for methylene carbon C4 for 10K and 300K polyisoprene in toluene-$d_8$ (90.6 MHz).

methylene carbons (see Figure 1) or 0.3 s for the methine carbon (see Figure 10).

It has been established for several flexible polymers in dilute solution that $T_1$ measurements are independent of molecular weight above a certain critical value.[23] We measured $T_1$ for two different molecular weights of polyisoprene in toluene and 2-pentanone. Figure 3 shows the results for the toluene solution (C4). Within experimental error there are no differences in the relaxation times for different molecular weight samples. Similar results were observed for C1 and C3 in toluene solutions and for all three carbons in 2-pentanone solutions (temperatures between 278 and 333 K were investigated). For other solvents measurements were made only for the 10K polymer, and it is these results that we will discuss below.

## Results and Discussion

Kramers' theory[13] provides a commonly used framework for quantitatively interpreting molecular dynamics in solution. This theory is based on the passage of a particle (the reacting chemical system) over a potential energy barrier. The solvent is treated as a random frictional force opposing passage across the barrier. Any spatial or temporal correlations in the solvent motion are neglected.

Helfand has applied Kramers' theory to the case of conformational transitions of polymers.[14] In the high-friction limit the rate constant is predicted to be

$$k = ((\gamma_a\gamma_b)^{0.5}/2\pi\zeta)\exp(-E_a/RT) \qquad (12)$$

where $\gamma_a$ is the curvature of the potential energy surface at the bottom of the initial well and $\gamma_b$ is the curvature at the top of the energy barrier for rotational motion. $\zeta$ is the friction coefficient of the solvent, and $E_a$ is the height of the energy barrier. The friction $\zeta$ is usually taken to be directly proportional to the zero-shear viscosity, $\eta$, of the solvent. We make the assumption that the correlation time measured in the NMR experiment is inversely proportional to the rate constant for isomerization. The temperature and viscosity dependence of $\tau_c$ is then predicted by Kramers' theory to be

$$\tau_c = A\eta\exp(E_a/RT) \qquad (13)$$

The prefactor $A$ is a constant, independent of temperature and viscosity. The temperature dependence of the viscosity can often be described with an Arrhenius form:

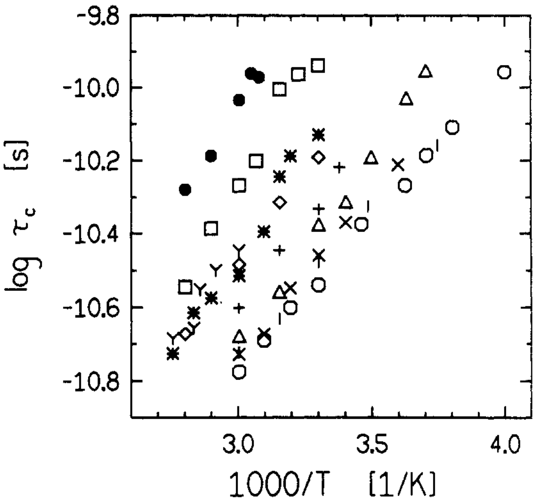

**Figure 4.** Temperature dependence of the correlation time, $\tau_c$, for methylene carbon C4 in all solvents: 2-pentanone (×); toluene (O); chloroform (|); cyclohexane (△); 1,4-dioxane (+); 1,1,2,2-tetrachloroethane (◇); $n$-hexadecane (*); *cis*-decalin (Y); squalane (□); Aroclor 1248 (●).

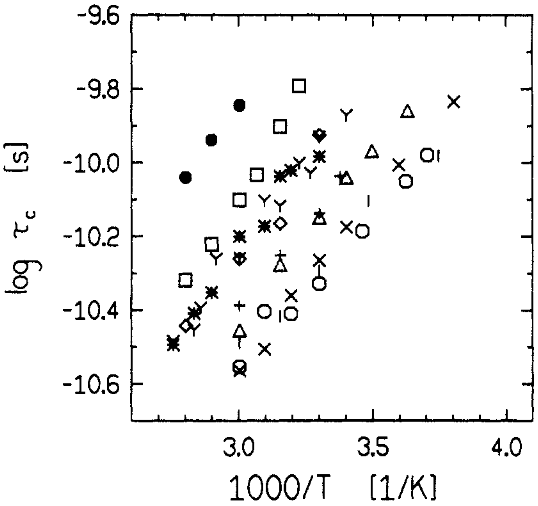

**Figure 5.** Temperature dependence of the correlation time, $\tau_c$, for methine carbon C3 in all solvents. The symbols are the same as in Figure 4.

$$\eta = \eta_0\exp(E_\eta/RT) \qquad (14)$$

Under these conditions

$$\tau_c = A'\exp[(E_a + E_\eta)/RT] \qquad (15)$$

where $A'$ is a constant. The experimental activation energy, $E_{\text{exptl}}$, obtained from a plot of $\ln\tau_c$ vs $1/T$ is therefore predicted to be the sum of the barrier height for conformational transitions and the viscous flow contribution:

$$E_{\text{exptl}} = E_a + E_\eta \qquad (16)$$

Figure 4 shows the temperature dependence of the effective correlation time $\tau_c$ of the methylene carbon C4 of 10K polyisoprene in 10 solvents. A similar plot for the methine carbon C3 is shown in Figure 5. Table III presents the average $E_{\text{exptl}}$ for the three backbone carbons, obtained as discussed in the previous paragraph. No systematic differences among the three carbons were observed. Also included are the solvent viscosities at 333 K and $E_\eta$. For solvents where the temperature dependence of the viscosity is not Arrhenius, $E_\eta$ was calculated from the best fit slope of a plot of $\ln\eta$ vs $1/T$ over the temperature range of interest.

Equation 13 indicates that at any given temperature

Table III
Activation Energies[a]

| solvent | $\eta^{333\ K}$, cP | $E_\eta$, kJ/mol | $E_{exptl}$, kJ/mol |
|---|---|---|---|
| 2-pentanone | 0.33 | 8.3 (0.3) | 17.2 (0.4) |
| toluene | 0.38 | 9.0 (0.3) | 15.5 (0.5) |
| chloroform | 0.39 | 7.4 (0.3) | 14.3 (0.6) |
| cyclohexane | 0.54 | 12.0 (0.3) | 19.1 (0.8) |
| 1,4-dioxane | 0.70 | 12.5 (0.3) | 18.5 (1.0) |
| tetrachloroethane | 0.98 | 12.0 (0.3) | 18.0 (1.4) |
| *n*-hexadecane | 1.59 | 15.0 (0.3) | 19.5 (1.9) |
| *cis*-decalin | 1.59 | 14.2 (0.3) | 19.0 (0.7) |
| squalane | 8.0 | 27.1 (2.6) | 25.5 (2.7) |
| Aroclor 1248 | 15.4 | 37.9 (4.4) | 23.9 (2.0) |

[a] Standard deviations are indicated in parentheses.

$\tau_c$ should be proportional to $\eta$. Figure 6 is a plot of log $\tau_c$ vs log $\eta$ for C4 at 333 K. If the prediction of Kramers' theory was correct, a straight line should be obtained with slope equal to unity. In fact, a straight line is obtained with a slope of 0.41 ± 0.02. Similar plots were obtained for C1 and C3, with slopes in the range indicated above.

Figure 6 clearly indicates that Kramers' theory in the high friction limit (eq 13) does not accurately describe the conformational dynamics of polyisoprene in dilute solution. At 333 K the correlation times vary by a factor of 5, while the viscosities span a factor of 46. One might ask if the assumption of the high-friction limit is too restrictive. Realistic estimates of the parameters in the full Kramers' expression[14] lead to the conclusion that the high-friction limit should be appropriate. In addition, there is no region in which the full Kramers' expression predicts a power law relationship (with the exponent not equal to 1) over a significant range in viscosity.

A power law relationship between the isomerization rate constant and the viscosity has been previously observed by Fleming and co-workers for the isomerization of stilbene in *n*-alkanes.[48] Similar behavior has been reported for the isomerizations of diphenylbutadiene,[49,50] 2-vinylanthracene derivatives,[51,52] and stilbene derivatives.[53] Fleming and co-workers suggested that the isomerization rate constant be written as

$$k = A\eta^{-\alpha} \exp(-E_a/RT) \tag{17}$$

with $\alpha < 1$. Writing this equation in terms of the correlation time

$$\tau_c = A'\eta^{\alpha} \exp(E_a/RT) \tag{18}$$

Figure 7 shows a plot of correlation times for C4 (all the data shown in Figure 5) in a format suggested by eq 18. The fact that a universal curve is obtained when $\tau_c$ is scaled by $\eta^{0.41}$ indicates that our data indeed follows this equation. The best fit slope through the points yields $E_a$ = 13 ± 2 kJ/mol. Activation energies for C1 and C3 were the same within experimental error.

A consequence of eq 18 is that the activation barrier for conformational transitions, $E_a$, cannot be determined from the temperature dependence of the dynamics in a single solvent (since $\alpha$ is not known in advance). Once $\alpha$ has been obtained, $E_a$ can be determined by

$$E_{exptl} = E_a + \alpha E_\eta \tag{19}$$

Figure 8 shows the activation energies for local motions of polyisoprene in the 10 solvents we studied. The circles show $E_{exptl}$ obtained as described in the text following eq 15. The plus symbols show the correct calculation of $E_a$ according to eq 19; the values obtained are very similar in all 10 solvents. The triangles show the calculation of $E_a$ assuming the Kramers' high-friction limit

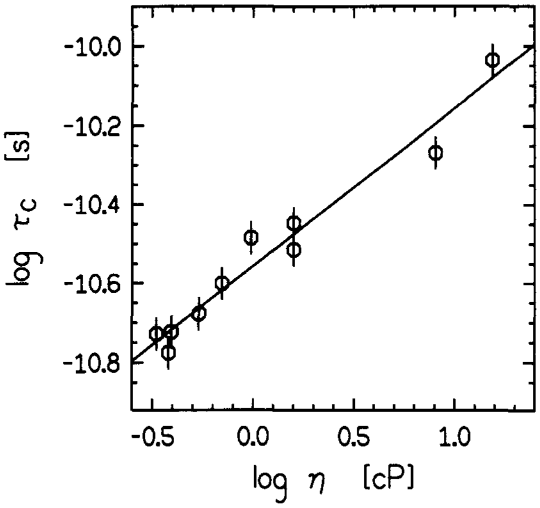

**Figure 6.** Viscosity dependence of the correlation time, $\tau_c$, for methylene carbon C4 at 333 K. The line is least-squares fit to the data with the slope 0.41.

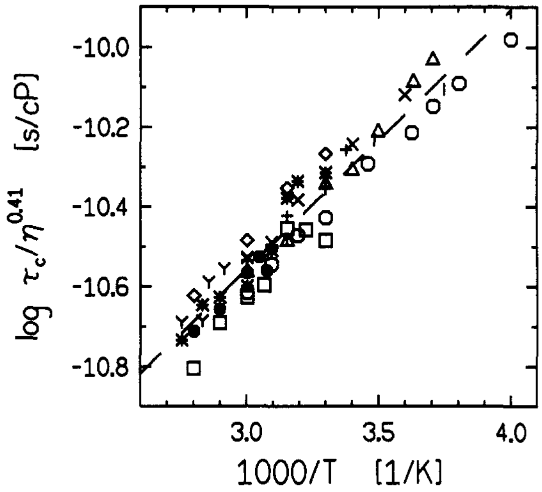

**Figure 7.** Temperature dependence of reduced correlation time ($\tau_c/\eta^{0.41}$) of methylene carbon C4. All data points shown in Figure 4 are included. Viscosities were evaluated from Table II.

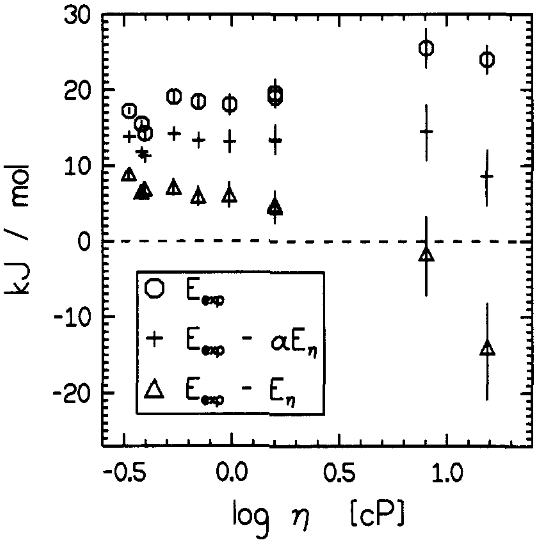

**Figure 8.** Solvent dependence of the experimental activation energy and the energy barriers calculated according to eq 16 (Kramers' theory) and eq 19. Solvents are identified by their viscosity at 333 K (Table III). Error bars are indicated. The energy barrier calculated according to eq 19 is essentially independent of solvent while the Kramers' result depends strongly on solvent and is sometimes negative.

(eq 16). Activation energies calculated in this way depend on the solvent viscosity. This is contrary to the usual interpretation of $E_a$ as an intramolecular potential barrier, which should not depend on the solvent identity in nonpolar systems. For solvents with high viscosities (and large $E_\eta$) the Kramers' calculation yields nonphysical negative values.

We turn now to the question of why $\alpha < 1$. A nonlinear dependence of relaxation times on viscosity can be discussed from two points of view. Kramers' theory is typically applied by assuming that the friction constant for an isomerization can be calculated from the zero-shear viscosity (a measurement made on slow time scales and large length scales). More general approaches assume that the friction constant should be related to either the frequency or wavevector dependence of the viscosity. Dote et al. have reviewed models that attribute nonlinearity to changes in the coupling between solvent and solute and they have proposed a new model of this type.[54] For this class of models, the critical feature is the relative length scales of solute and solvent motion. It is worth noting that the highly viscous solvents used in this study are considerably larger than the polyisoprene repeat unit. Grote and Hynes have taken the other approach, considering how an intrinsic frequency dependence in the friction would affect the rate of a chemical reaction.[15] It is difficult to separate the influences of length scales and time scales, so neither approach can be eliminated from consideration at the present time. Since the Grote–Hynes theory is formulated for activated processes, we will discuss our results in terms of this approach.

Grote and Hynes[15] have generalized Kramers' theory by allowing the solvent friction $\zeta$ to be frequency dependent and not simply proportional to the zero-shear viscosity. They showed that the friction coefficient applicable to a particular chemical reaction can be much smaller than the friction coefficient calculated from the zero-shear viscosity. For reactions with steep energy barriers the time spent diffusing across the barrier becomes very small. Many of the low-frequency solvent motions that contribute to the zero-shear viscosity will be too slow to affect the reactive motion. This effect will be strongest for reactions with steep energy barriers. Bagchi and Oxtoby[55] have applied Grote–Hynes theory to describe the isomerization of stilbene in *n*-alkanes. They treated the frequency dependence of the friction using expressions developed by Zwanzig and Bixon and by Montgomery and Berne.[56] The solvents were modeled as a viscoelastic continuum with a single relaxation time. Using the Grote–Hynes theory, Bagchi and Oxtoby found isomerization rates that have a power law dependence on the viscosity, in agreement with eq 17 and our results.

The exponent $\alpha$ depends on the moment of inertia and size of the isomerizing unit and on the curvature of the potential energy surface at the top of barrier. Smaller size, a smaller moment of inertia, and a higher barrier all lead to a smaller value of $\alpha$. These parameters are expected to vary from polymer to polymer, so a universal value of $\alpha$ is not expected. We will not attempt to calculate $\alpha$ for polyisoprene since the nature of the isomerizing unit is not precisely known. In addition, uncertainty about solvent properties makes such a calculation difficult even for small molecules.[55]

Within the context of the Grote–Hynes theory, the breakdown of Kramers' theory is fundamentally due to the fact that the time scales for polymer and solvent motion are not cleanly separable. This can be qualitatively seen in Figure 9, where we show the correlation times for conformational dynamics along with correlation times for solvent rotation.[57] Particularly at high viscosities, the time scales for polymer and solvent motion are very similar. Kramers' theory assumes that solvent–polymer collisions are uncorrelated in space and time. However, motion near the top of the isomerization barrier occurs on a very short time scale (picoseconds or less). On these time scales, correlations in collisions may indeed be significant.

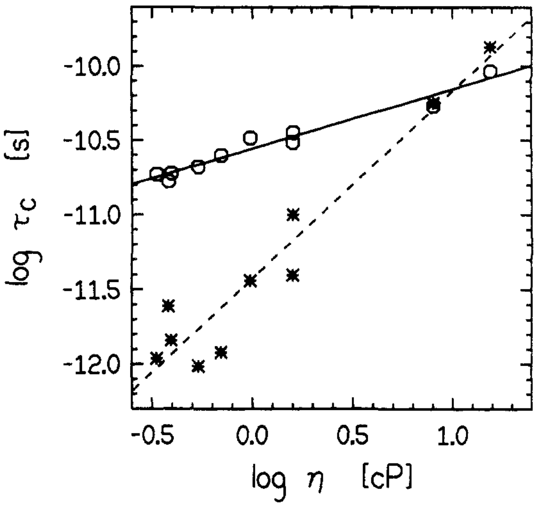

**Figure 9.** Viscosity dependence of the correlation time, $\tau_c$, for solvent molecules at 333 K (*). Data for polymer methylene carbon C4 from Figure 6 are also included (○). The lines are least-squares fits. The solvent $\tau_c$s were determined from $^{13}$C $T_1$s of nondeuterated solvents according to eq 8. For solvents with more than one chemically distinct carbon atom, the correlation time for the methine or methylene carbon which best reflects motions of the center of molecule is reported.

The scaling of $\tau_c$ with $\eta^{0.41}$ shown in Figure 6 is not expected to hold for arbitrarily large solvent viscosities. For example, if a series of isoprene oligomers were used as solvents, the solvent viscosity would increase with the oligomer length. However, eventually $\tau_c$ would become independent of solvent length and viscosity (it is known that $\tau_c$ is independent of molecular weight at high molecular weights[6]). The fact that relatively flexible solvent molecules (e.g., squalane and hexadecane) and relatively rigid solvent molecules (e.g., decalin and Aroclor 1248) lie on the same line in Figure 6 suggests that solvent flexibility is not an important parameter for the solvents studied in this work.

**$nT_1$ Ratios.** The chemical sensitivity of NMR experiments provides the opportunity to study fine details of molecular dynamics, even on length scales shorter than a single repeat unit. Equation 8 predicts that if the correlation times and bond lengths for different C–H vectors in the chain backbone are the same, then $nT_1$ should be the same for the backbone carbons. This expectation that the correlation times for different C–H vectors should be the same is sometimes referred to as the $nT_1$ rule.

The $nT_1$ rule is nearly always valid for dilute solutions of vinyl polymers[23,30,44,58] and polymers with backbone heteroatoms, such as poly(styrene oxide),[59] poly(phenylthiirane),[60] and poly(styrene peroxide).[61] This is not the case for polymers with repeat units that contain relatively hard and soft segments, such as poly(butylene terephthalate) and similar polyesters.[62–64] Previous authors have noted that the $nT_1$ rule fails for *cis*-polybutadiene[5,65] and *cis*-polyisoprene[5,12] but apparently works for *trans*-polybutadiene[65] and *trans*-polyisoprene,[12] although very little information is available for the trans polymers.

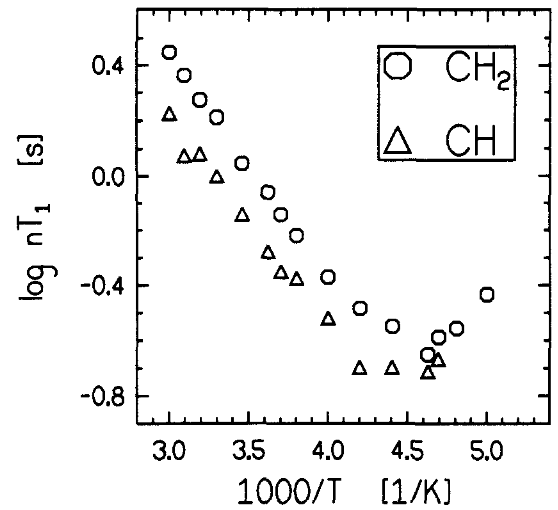

**Figure 10.** Temperature dependence of $nT_1$ for methylene carbon C4 and methine carbon C3 at 90.6 MHz.

**Table IV**
**$nT_1$ Ratios**[a]

| solvent | temp range, K | C4/C3 | C4/C1 |
|---|---|---|---|
| 2-pentanone | 278–333 | 1.54 (0.06) | 1.12 (0.10) |
| toluene | 270–333 | 1.65 (0.13) | 1.15 (0.04) |
| chloroform | 267–333 | 1.61 (0.09) | 1.14 (0.05) |
| cyclohexane | 275–333 | 1.71 (0.16) | 1.17 (0.04) |
| 1,4-dioxane | 296–333 | 1.57 (0.05) | 1.21 (0.03) |
| tetrachloroethane | 303–357 | 1.66 (0.18) | 1.24 (0.09) |
| *n*-hexadecane | 313–363 | 1.68 (0.18) | 1.10 (0.14) |
| *cis*-decalin | 333–363 | 1.58 (0.11) | 1.36 (0.10) |
| squalane | 310–357 | 1.47 (0.13) | 1.17 (0.09) |
| Aroclor 1248 | 333–357 | 1.71 (0.09) | 1.18 (0.10) |
| all solvents | | 1.62 (0.14) | 1.18 (0.11) |

[a] Columns C4/C3 and C4/C1 show average ratios of $nT_1$ values for the indicated carbon nuclei. Standard deviations are in parentheses.

Figure 10 shows the temperature dependence of $nT_1$ for carbons C3 and C4 of polyisoprene in toluene. The $nT_1$ values for the two carbons are not the same, indicating that the $nT_1$ rule is not followed. The ratio of the two $nT_1$ values is constant within experimental error, independent of temperature. The ratio of $nT_1$ values for C1 and C4 is also independent of temperature and not equal to one. Similar behavior was observed in all other solvents. In Table IV we show the values for the ratios in all solvents, averaged over temperature. There are no significant differences among the solvents.

There are four factors that possibly contribute to the breakdown of the $nT_1$ rule for polyisoprene in dilute solution: (i) Small differences in the methine and methylene C–H bond lengths can affect the $nT_1$ ratios. A possible difference of 0.01 Å between the two bond lengths[66] results in only a 5% difference in $nT_1$. (ii) Dipolar coupling to nonbonded protons has sometimes been used as an explanation.[6] Experiments by Schaefer indicate that up to 20% of the methine carbon relaxation may be due to this in bulk polyisoprene.[37] It is likely that this value is smaller in dilute solutions. In addition, all carbon $T_1$ values are likely to be shortened if this mechanism is important, so calculating ratios of $T_1$ values should partially eliminate this problem. (iii) Anisotropic motion due to specific, cooperative conformational transitions could account for the observed ratios. Gronski has proposed such a mechanism for *cis*-polybutadiene.[67] (iv) High-frequency librations of different amplitudes on different C–H vectors could account for the observed ratios. Recent work by Dejean de la Batie et al. has discussed this possibility in regard to bulk polyisoprene.[5]

We believe that the third and fourth factors listed above are the only explanations consistent with $nT_1$ ratios significantly different from one. Thus the observed $nT_1$ ratios indicate real differences in the dynamics of the three C–H vectors monitored in the NMR experiment.

The fact that the $nT_1$ ratios do not depend on the solvent offers indirect evidence that the mechanisms for segmental motion of polyisoprene are determined predominantly by the chemical structure of the repeat unit. There is no evidence that the chemical identity of the solvent affects the mechanism, at least in the absence of strong solute/solvent interactions (such as hydrogen bonding). The time scale for the dynamics is determined by the viscosity as discussed earlier. These results encourage the possibility of modeling dilute solution dynamics by considering the solvent as a continuum with only the viscosity and temperature as variables.

In work to be published, we will show the important influence of high-frequency librations on the observed solution $T_1$ values.[68] Qualitatively, we can infer that the bulky $CHCCH_3$ group restricts the motion of the methine carbon C3 more than the relatively mobile methylene groups. Steric interactions with the methyl group presumably hinder motions of C1 more than C4. Recently it was shown in our laboratory that Brownian dynamics computer simulations of polyisoprene in solution can semiquantitatively reproduce the $nT_1$ ratios presented here.[69] These simulations should allow a detailed analysis of the molecular dynamics of this system.

Other authors have measured $nT_1$ ratios for polyisoprene in dilute solutions.[5,12] Their results are in fairly good agreement with ours. Dejean de la Batie et al.[5] measured $^{13}$C $T_1$s in bulk polyisoprene (92% cis) and found $nT_1$ ratios of 1.42 for C4/C3 and 1.28 for C4/C1.[70] The $nT_1$ ratios for bulk polyisoprene are not too different from those obtained in solution. This suggests that the mechanisms for local dynamics in solution and in the bulk may be similar.

## Comparison to Previous Work

**NMR Experiments.** To the best of our knowledge, only poly(ethylene oxide) (PEO) has been studied with NMR techniques using solvents spanning a wide viscosity range. Liu and Anderson[10] have measured $^1$H $T_1$s for PEO at a single temperature in a series of halogenated solvents covering the viscosity range 0.4–7.2 cP. They concluded that segmental dynamics are predominantly governed by the local viscosity, which in turn is related, but not necessarily equal, to the solvent viscosity.

Monnerie and co-workers have reached a similar conclusion.[9] They measured the $^{13}$C spin–lattice relaxation times of PEO at 303 K in a series of 12 solvents similar to those used by Liu and Anderson, covering the same viscosity range. The correlation times, $\tau_c$, derived from the $^{13}$C experiments depended on viscosity more weakly than the Stokes–Einstein prediction ($\tau_c \propto \eta$). The results were discussed in terms of Magee's model,[71] which assumes a nonlinear relationship between the correlation time of the solute and the macroscopic solvent viscosity.

Magee's model pictures a spherical solute surrounded by a structured solvent layer. The interactions between the solute and this solvent shell and between this structured complex and the bulk solvent are considered. The model predicts that a plot of $1/\tau_c$ as a function of $1/\eta$ should yield a straight line. The slope of this line is related to the volume of the structured region and the intercept

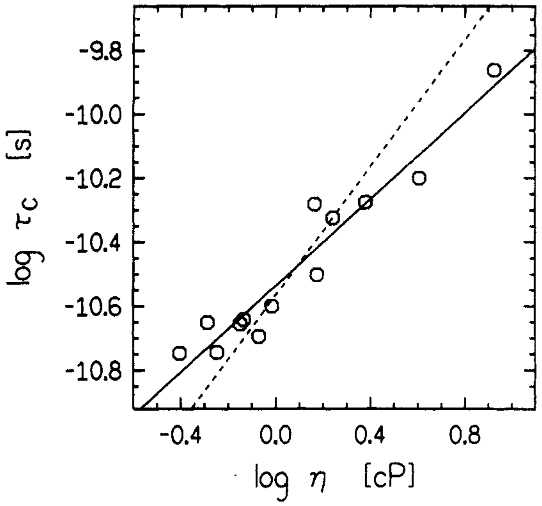

**Figure 11.** Viscosity dependence of the correlation time for PEO (ref 9) plotted in the same format as Figure 6. The solid line going through the data is a least-squares fit to the data with the slope 0.67. A dashed line with slope 1 is shown for comparison.

is the limiting correlation time for highly viscous solvents.

We have investigated whether the PEO data might be equally well described by a power law relationship between $\tau_c$ and $\eta$, as suggested by the Grote–Hynes theory. Figure 11 shows the data from ref 9 replotted in this format. The points are well approximated by a straight line with slope $\alpha = 0.67$. Liu and Anderson's results can similarly be replotted, leading to a straight line with slope $\alpha = 0.69$. We have determined that our data (Figure 6) does not yield a straight line when plotted as $1/\tau_c$ vs $1/\eta$, as suggested by Magee's theory.

Although the Grote–Hynes and Magee models both predict a nonlinear relationship between the correlation time and the solvent viscosity, the theories have quite different foundations. The Grote–Hynes model considers the frequency of motion at the top of the potential barrier. The isomerizing group experiences less friction than that predicted by the zero-shear viscosity because its motion across the potential barrier is very rapid. The Magee model assumes that the interaction between the isomerizing segment of the chain and the closest solvent molecules is constant; the limiting correlation time at high viscosity depends only on the size of the moving particle and the solvent molecules. The data shown in Figures 6 and 11 do not indicate any symptoms of this saturation effect at high viscosities, as predicted by the Magee theory. On both theoretical and experimental grounds, we believe that the Grote–Hynes approach, which invokes a dynamic relationship between the solute and solvent, is more appropriate for describing solvent/polymer interactions than Magee's static picture.

Another feature of Grote–Hynes theory, as applied by Bagchi and Oxtoby, is that it rationalizes the use of eq 17–19, which leads to reasonable values for the activation energies for segmental motion in polyisoprene (see Figure 8). We could not check this for PEO since those NMR studies were performed at only one temperature. Many other previous investigators have *assumed* that Kramers' theory was valid and used eq 16 to calculate the height of a potential energy barrier. In some cases the activation energies thus obtained have been quite low, even equal to zero.[72] The Grote–Hynes theory provides an explanation for this behavior if $\alpha < 1$ for these polymers. Experiments using several different solvents with different viscosities are required to determine if $\alpha < 1$.

**Optical Experiments.** Earlier experiments in our laboratory have investigated local segmental dynamics of polyisoprene in dilute solution by using time-resolved optical spectroscopy. In these experiments the motion of an anthracene chromophore covalently bonded into the chain backbone was observed.[1] The principal conclusions of that work were as follows: (1) the local dynamics of polyisoprene were dependent on molecular weight in a $\Theta$ solvent but not in good solvents, (2) the segmental dynamics were slower in the $\Theta$ solvent than in good solvents, and (3) $\tau_c$ scaled roughly linearly with solvent viscosity in good solvents. The first two effects were explained by considering changes in the local segment concentration due to global configuration changes induced by changing the solvent quality.

The results from the optical experiments are different from those in the present work. The NMR experiments were carried out for polyisoprene samples with the same range of molecular weight by using some of the same solvents, toluene (good) and 2-pentanone ($\Theta$ solvent). The NMR experiments show that $\tau_c$ scales with $\eta^{0.41}$ with no differences observed for good and $\Theta$ solvents. Also, the NMR results indicate that $\tau_c$ does not depend on molecular weight in any solvents studied (see Figure 4 and related discussion). This feature is characteristic of NMR studies of synthetic polymers[23] when molecular weight exceeds a critical value, usually corresponding to a degree of polymerization between 30 and 100.

We interpret the differences between the two experiments in the following manner. Although the two experimental techniques are both sensitive to local dynamics, they monitor dynamics on different length scales, as suggested by Friedrich et al.[8] In polyisoprene, NMR experiments sense motions on the scale of 1–2 monomer units, while the optical experiments probe motions of 4–8 monomer units.[2,8,73,74] This is consistent with the difference between absolute $\tau_c$ values measured by the two experiments (e.g., $\tau_{c,\mathrm{optical}}$ is 14 times longer than $\tau_{c,\mathrm{NMR}}$ in toluene at 333 K). The larger length scales involved in the optical experiments mean that these experiments will be more sensitive to steric interactions with other chain segments when global chain dimensions change in response to solvent quality. The difference in the viscosity exponent, $\alpha$, can be understood in terms of Grote–Hynes theory. Reorientation of the optical probe involves a larger isomerizing group with a larger moment of inertia relative to the motions involved in the NMR experiments, and also involves a lower activation energy. All of these factors cause $\alpha$ to be larger in the optical experiments.

## Summary

Kramers' theory in the high-friction limit is often assumed to be the appropriate theoretical framework for discussing the local segmental motions of synthetic polymers in dilute solution. By performing experiments in solvents with a wide range of viscosities, we have shown that this assumption is incorrect for polyisoprene solutions. Indeed, it may be that Kramers' theory is inappropriate for describing the local dynamics of many synthetic polymers. We have shown that the application of Kramers' theory where it does not apply can lead to serious errors when potential energy barriers for conformational dynamics are calculated from temperature-dependent data. This in turn may lead to erroneous conclusions about the mechanisms of the local motions.

The Grote–Hynes theory and calculations by Bagchi and Oxtoby provide an alternate framework for discussing conformational dynamics. This approach emphasizes that the effective friction experienced in an isomerization depends upon the frequency at which the barrier is crossed. This approach qualitatively explains our NMR results and provides a way to compare them with previous measurements on the same system with time-resolved optical spectroscopy. In particular, the Grote–Hynes theory rationalizes why the correlation time for conformational transitions scales as $\eta^{0.41}$, instead of the first power dependence predicted by Kramers' theory.

None of the experimental results reported here provide any evidence for the importance of specific polymer/solvent interactions. Our NMR results fall on a universal curve such that only the viscosity and temperature need be specified to predict the correlation time, independent of the solvent identity. The ratios of correlation times for the motions of different C–H vectors attached to the chain backbone also do not depend on the solvent identity. We expect that these conclusions about the role of the solvent in local segmental dynamics may not be appropriate for more polar polymer/solvent systems or systems where hydrogen bonding occurs.

**Acknowledgment.** This research was supported by the National Science Foundation (Grant DMR-8822076) and the Graduate School of the University of Wisconsin. D.J.G. thanks IBM for fellowship support. NMR experiments were performed in the Instrument Center of the Department of Chemistry, University of Wisconsin, and we thank the staff for assistance. We also thank Alan Jones, Alan English, Thomas Farrar, Daniel Kivelson, Eugene Helfand, and Frank Blum for helpful discussions.

## References and Notes

(1) Waldow, D. A.; Johnson, B. S.; Hyde, P. D.; Ediger, M. D.; Kitano, T.; Ito, K. *Macromolecules* **1989**, *22*, 1345.
(2) Hyde, P. D.; Ediger, M. D.; Kitano, T.; Ito, K. *Macromolecules* **1989**, *22*, 2253.
(3) Veissier, V.; Viovy, J. L.; Monnerie, L. *Polymer* **1989**, *30*, 1262.
(4) Sasaki, T.; Yamamoto, M.; Nishijima, Y. *Macromolecules* **1988**, *21*, 610.
(5) Dejean de la Batie, R.; Laupretre, F.; Monnerie, L. *Macromolecules* **1989**, *22*, 122.
(6) Denault, J.; Prud'homme, J. *Macromolecules* **1989**, *22*, 1307.
(7) Mashimo, S. *Macromolecules* **1976**, *9*, 91.
(8) Friedrich, C.; Laupretre, F.; Noel, C.; Monnerie, L. *Macromolecules* **1981**, *14*, 1119.
(9) Lang, M. C.; Laupretre, F.; Noel, C.; Monnerie, L. *J. Chem. Soc., Faraday Trans. 2* **1979**, *75*, 349.
(10) Liu, K. J.; Anderson, J. E. *Macromolecules* **1970**, *3*, 163.
(11) Lodge, T. P.; Schrag, J. L. *Macromolecules* **1984**, *17*, 352.
(12) Hatada, K.; Kitayama, T.; Terawaki, Y.; Tanaka, Y.; Sato, H. *Polym. Bull. (Berlin)* **1980**, *2*, 791.
(13) Kramers, H. A. *Physica* **1940**, *7*, 284.
(14) Helfand, E. *J. Chem. Phys.* **1971**, *54*, 4651.
(15) Grote, R. F.; Hynes, J. T. *J. Chem. Phys.* **1980**, *73*, 2715.
(16) Paul, D. R.; Garcin, M.; Garmon, W. E. *J. Appl. Polym. Sci.* **1976**, *20*, 609.
(17) Tsunashima, Y.; Hirata, M.; Nemoto, N.; Kurata, M. *Macromolecules* **1987**, *20*, 1992.
(18) Adachi, K.; Imanishi, Y.; Shinkado, T.; Kotaka, T. *Macromolecules* **1989**, *22*, 2391.
(19) Hadjichristidis, N.; Roovers, J. E. L. *J. Polym. Sci., Polym. Phys. Ed.* **1974**, *12*, 2521.
(20) Merchak, P. A. Ph.D. Thesis, University of Wisconsin, 1987.
(21) Stokich, T. M. Ph.D. Thesis, University of Wisconsin, 1988.
(22) Harris, J. S. *Prod. Eng.* December **1954**, *25*, 163.
(23) Heatley, F. *Prog. Nucl. Magn. Reson. Spectrosc.* **1979**, *13*, 47 and references therein.
(24) Craik, D. C.; Levy, G. C. *Top. Carbon-13 NMR Spectrosc.* **1984**, *4*, 239.
(25) Shaw, D. *Fourier Transform NMR Spectroscopy*; Elsevier: Amsterdam, 1976.
(26) Duch, M. W.; Grant, D. M. *Macromolecules* **1970**, *3*, 165.
(27) Sato, H.; Ono, A.; Tanaka, Y. *Polymer* **1977**, *18*, 580.
(28) Levitt, M. H. *Prog. Nucl. Magn. Reson. Spectrosc.* **1986**, *18*, 61.
(29) Lyerla, J. R.; Levy, G. C. *Top. Carbon-13 NMR Spectrosc.* **1974**, *1*, 79.
(30) Heatley, F. *Annu. Rep. NMR Spectrosc.* **1986**, *17*, 179 and references therein.
(31) Abragam, A. *The Principles of Nuclear Magnetism*; Clarendon Press: Oxford, 1961; Chapter VIII.
(32) Lenk, R. *Fluctuations, Diffusion and Spin Relaxation*; Elsevier: Amsterdam, 1986; p 7.
(33) Kubo, R.; Toda, M.; Hashitsume, H. *Statistical Physics II: Nonequilibrium Statistical Mechanics*; Springer-Verlag: Berlin, 1985; p 42.
(34) Meiboom, S.; Gill, D. *Rev. Sci. Instrum.* **1958**, *29*, 688.
(35) Farrar, T. C.; Becker, E. D. *Pulse and Fourier Transform NMR*; Academic Press: New York, 1971; p 27.
(36) English, A. D.; Dybowski, C. R. *Macromolecules* **1984**, *17*, 446.
(37) Schaefer, J. *Macromolecules* **1972**, *5*, 427.
(38) Levine, Y. K.; Partington, P.; Roberts, G. C. K. *Mol. Phys.* **1973**, *25*, 497.
(39) Heatley, F.; Walton, I. *Polymer* **1976**, *17*, 1019.
(40) Inoue, Y.; Nishioka, A.; Chujo, R. *J. Polym. Sci., Polym. Phys. Ed.* **1973**, *11*, 2237.
(41) Jones, A. A.; Stockmayer, W. H. *J. Polym. Sci., Polym. Phys. Ed.* **1977**, *15*, 847.
(42) Bendler, J. T.; Yaris, R. *Macromolecules* **1978**, *11*, 650.
(43) Hall, C. K.; Helfand, E. *J. Chem. Phys.* **1982**, *77*, 3275.
(44) Dejean de la Batie, R.; Laupretre, F.; Monnerie, L. *Macromolecules* **1988**, *21*, 2045.
(45) Schaefer, J. *Macromolecules* **1973**, *6*, 882.
(46) Farrar, T. C.; Adams, B. R.; Grey, G. C.; Quintero-Arcaya, R. A.; Zuo, Q. *J. Am. Chem. Soc.* **1986**, *108*, 8190.
(47) Komoroski, R. A. In *High Resolution NMR Spectroscopy of Synthetic Polymers in Bulk*; Komoroski, R. A., Ed.; VCH Publishers: Deerfield Beach, FL, 1986; p 28.
(48) Courtney, S. H.; Fleming, G. R. *J. Chem. Phys.* **1985**, *83*, 215.
(49) Velsko, S. P.; Fleming, G. R. *J. Chem. Phys.* **1982**, *76*, 3553.
(50) Keery, K. M.; Fleming, G. R. *Chem. Phys. Lett.* **1982**, *93*, 322.
(51) Flom, S. R.; Nagarajan, V.; Barbara, P. F. *J. Phys. Chem.* **1986**, *90*, 2085.
(52) Brearley, A. M.; Flom, S. R.; Nagarajan, V.; Barbara, P. F. *J. Phys. Chem.* **1986**, *90*, 2092.
(53) Rothenberger, G.; Negus, D. K.; Hochstrasser, R. M. *J. Chem. Phys.* **1983**, *79*, 5360.
(54) Dote, J. L.; Kivelson, D.; Schwartz, R. N. *J. Phys. Chem.* **1981**, *85*, 2169.
(55) Bagchi, B.; Oxtoby, D. W. *J. Chem. Phys.* **1983**, *78*, 2735.
(56) Zwanzig, R.; Bixon, M. *Phys. Rev. A* **1970**, *2*, 2005. Montgomery, J. A.; Berne, B. J. *J. Chem. Phys.* **1977**, *66*, 2770.
(57) According to reference 55, a more relevant comparison is between the time spent crossing the barrier (which is less than $\tau_{c,\mathrm{polymer}}$) and the solvent relaxation time ($\approx\tau_{c,\mathrm{solvent}}$).
(58) Bovey, F. A.; Jelinski, L. W. *J. Phys. Chem.* **1985**, *89*, 571 and references therein.
(59) Matsuo, K.; Stockmayer, W. H.; Mashimo, S. *Macromolecules* **1982**, *15*, 606.
(60) Cais, R. E.; Bovey, F. A. *Macromolecules* **1977**, *10*, 752.
(61) Cais, R. E.; Bovey, F. A. *Macromolecules* **1977**, *10*, 169.
(62) Jelinski, L. W.; Dumais, J. J.; Watnick, P. I.; Engel, A. K.; Sefcik, M. D. *Macromolecules* **1983**, *16*, 409.
(63) Henrichs, P. M.; Hewitt, J. M.; Russell, G. A.; Sandhu, M. A.; Grashof, H. R. *Macromolecules* **1981**, *14*, 1770.
(64) Tekely, P.; Laupretre, F.; Monnerie, L. *Macromolecules* **1983**, *16*, 415.
(65) Gronski, W.; Murayama, N. *Makromol. Chem.* **1976**, *177*, 3017.
(66) *Tables of Interatomic Distances and Configuration in Molecules and Ions*; Special Publication Nos. 11 and 18; The Chemical Society: London, 1958 and 1965.
(67) Gronski, W. *Makromol. Chem.* **1977**, *178*, 2949.
(68) Gisser, D. J.; Glowinkowski, S.; Ediger, M. D., to be published in *Macromolecules*.
(69) Adolf, D. B.; Ediger, M. D. in *Computer Simulation of Polymers*; Roe, R. J., Ed.; Prentice-Hall: Englewood Cliffs, NJ, to be published.
(70) These values were calculated by using data from ref 5, collected at a resonance frequency of 25 MHz over the temperature range 329–383 K.
(71) Magee, M. D. *J. Chem. Soc., Faraday Trans. 2* **1974**, *70*, 929.
(72) Hermann, G.; Weill, G. *Macromolecules* **1975**, *8*, 171.
(73) Viovy, J. L.; Frank, C. W.; Monnerie, L. *Macromolecules* **1985**, *18*, 2606.
(74) Hyde, P. D.; Ediger, M. D. *J. Chem. Phys.* **1990**, *92*, 1036.
(75) *International Critical Tables*; Washburn, E. W.; West, C. J.; Dorsey, N. E.; Ring, M. D., Eds.; McGraw-Hill: New York, 1930; Vol. VII, p 211.
(76) Barlow, A. J.; Lamb, J.; Matheson, A. J. *Proc. R. Soc. London A* **1966**, *292*, 322.

(77) Viswanath, D. S.; Natarajan, G. *Data Book on the Viscosity of Liquids*; Hemisphere Publishing: New York, 1989.

(78) *Landolt-Bornstein, Zahlenwerte und Funktionen*; Springer-Verlag: Berlin, 1969; Band II, Teil 5, p 217.

# Notes

## Glass Transition Temperatures of Polymethacrylates with Alicyclic Side Groups

JIMMY W. MAYS*

*Department of Chemistry, University of Alabama at Birmingham, Birmingham, Alabama 35294*

EKATERINI SIAKALI-KIOULAFA AND NIKOS HADJICHRISTIDIS

*Department of Chemistry, University of Athens, Athens 106 80, Greece*

*Received December 18, 1989;*
*Revised Manuscript Received February 5, 1990*

### Introduction

The presence of long flexible *n*-alkyl substituents has a profound impact on the glass transition temperature $T_g$ of various classes of macromolecules, including polyolefins,[1,2] poly(*p*-alkylstyrenes),[3] polyacrylates,[4] and polymethacrylates.[4,5] As the length of the *n*-alkyl side chain increases, $T_g$ decreases within each of these families of polymers.

The effect of varying the size of alicyclic ring substituents on $T_g$ has not, with one exception, been explored. Wilson and Simha[6] previously determined the $T_g$'s of poly(cyclohexyl methacrylate) and poly(cyclopentyl methacrylate) by volume expansion. In this note we report $T_g$ for a series of six fractionated high molecular weight polymethacrylates with ring sizes ranging from cyclo butyl to cycloheptadecyl.

### Experimental Section

Monomers and polymers were synthesized by methods that were reported previously.[7] The polymers were fractionated by addition of methanol to dilute toluene solutions (<1% w/w). Molecular weights and polydispersities were obtained by low-angle laser light scattering (LALLS), osmometry, and size exclusion chromatography (SEC), as previously described.[7] Molecular characteristics of the selected fractions are presented in Table I.

Tacticities were determined by $^{13}C$ NMR measurements in $CDCl_3$ at 25 °C. The triad concentrations were evaluated from the intensities of peaks corresponding to the carbonyl carbon.

A Perkin-Elmer DSC-2 differential scanning calorimeter was used to measure $T_g$. Calibration of this instrument was based on an indium standard. Sample sizes of 5–10 mg and a heating rate of 5 °C min$^{-1}$ were employed.

### Results and Discussion

Table II lists the tacticities and glass transition temperatures of the polymethacrylates. For materials prepared under identical conditions (AIBN initiation, 50 °C), the tacticity is independent of the size of the alicyclic side group.

On the other hand, $T_g$ is affected by ring size. As the alicyclic ring becomes larger, $T_g$ decreases from the value of 78 °C found for PCBM and then appears to level off (at 56 °C) for the largest rings investigated ($C_{12}$ and $C_{17}$). A plot of $T_g$ versus the number of carbons in the side group is presented in Figure 1 for both alicyclic and *n*-alkyl-substituted polymethacrylates. The impact on $T_g$ of increasing ring size is quite modest compared to the very large decreases observed with *n*-alkyl substituents with the same number of carbons.

$T_g$ is known to increase with an increase in substituent size for rigid substituents because of the increased barrier to rotation about backbone bonds.[8,9] However, for flexible side chains such as *n*-alkyl, only the first methylene group is attached rigidly to the methacrylate backbone. The remainder of *n*-alkyl chains can avoid rotating backbone units; thus the addition of these groups has the effect of decreasing $T_g$ ("internal plasticization").[8,9] Although alicyclic side groups are not rigid, their cyclic structure moves the center of mass of the side group closer to the polymer backbone and the bulkiness of the substituent becomes important with regard to $T_g$. The ali-

**Table I**
**Molecular Weights and Polydispersities of Fractionated Polymethacrylates**

| polymer | $10^{-4}\bar{M}_w$[g] | $10^{-4}\bar{M}_n$[h] | $\bar{M}_w/\bar{M}_n$[i] | $\bar{M}_z/\bar{M}_w$[i] |
|---|---|---|---|---|
| PCBM[a] | 13.9 | 12.1 | 1.3 | 1.3 |
| PCPM[b] | 11.0 | 10.4 | 1.2 | 1.2 |
| PCOM[c] | 12.1 | 9.1 | 1.4 | 1.3 |
| PCDM[d] | | 33.4[j] | 1.7 | 1.6 |
| PCDDM[e] | 9.8 | 7.3 | 1.4 | 1.5 |
| PCHDM[f] | | 12.2[j] | 1.6 | 1.4 |

[a] Poly(cyclobutyl methacrylate). [b] Poly(cyclopentyl methacrylate). [c] Poly(cyclooctyl methacrylate). [d] Poly(cyclodecyl methacrylate). [e] Poly(cyclododecyl methacrylate). [f] Poly(cycloheptadecyl methacrylate). [g] LALLS. [h] Osmometry. [i] SEC. [j] Via SEC based on a polystyrene calibration.

**Table II**
**Tacticity and Glass Transition Temperatures of Polymethacrylates**

| | | tacticity, % | | |
|---|---|---|---|---|
| polymer | $T_g$, °C | mm | mr + rm | rr |
| PCBM | 78 | 3 | 32 | 65 |
| PCPM | 75 | 2 | 32 | 66 |
| PCOM | 73 | 3 | 34 | 63 |
| PCDM | 58 | 3 | 30 | 67 |
| PCDDM | 56 | 3 | 34 | 63 |
| PCHDM | 56 | 2 | 31 | 67 |